

# Experimental Investigation of Seismic-Earth-Slope Displacement by a Logarithmic Spiral Failure Slide

by

Tomoyuki SAWADA\*, Sumio G. NOMACHI\*\*, Isao IKEURA\*\*\*  
and Toshiyuki MITACHI\*\*\*\*

(Received November 30, 1990)

## Abstract

If the factor of safety is less than unity, then the slope is considered unsafe. This is certainly true under static gravity loading condition. However, under an earthquake loading, the reduction in factor of safety only exists during very short periods of time for which large inertia forces are induced. Further, during an earthquake, the induced inertia forces will also alternate in direction and magnitude numerous times, only those inertia forces that exceed the failure limit of the slope will induce some displacements. All these driving forces will be rapidly removed both during and at the end of an earthquake. As soon as the ground motion ceases, no further displacement will occur unless the soil strength has been degraded significantly by the cyclic loading. The overall effect of an earthquake on the slope is therefore the accumulation of displacements of the failed section<sup>(6,7)</sup>. If these accumulated displacements are sufficiently large, the slope may be considered to have failed.

In this paper, to apply Newmark's concept, a failure mechanism and its corresponding yield acceleration must be determined first from which the overall displacements of a failed slope under earthquake loads can be assessed<sup>(6)</sup>.

These calculations can best be achieved by the following steps :

1. Calculate the yield acceleration at which the slippage is just to occur.
2. Apply various values of pseudo-static force to the slope. These values are obtained from a discretized accelerogram of an actual or simulated earthquake.
3. Once the yield acceleration and accelerogram of an earthquake are known, it is a simple matter to calculate the time history of velocity of the sliding soil mass of a given slope. The magnitude of the displacements can then be evaluated by integrating all the positive velocity.

The computation of the yield acceleration based on the upper bound technique of limit analysis of perfect plasticity has been reported elsewhere.<sup>1)2)</sup>

---

\* Assoc. Professor, Dept. of Civil Engineering, Tomakomai National College of Technology, Hokkaido.

\*\* Professor, School of Industrial Technology, Dept. of Civil Engineering, Nihon University, Chiba.

\*\*\* Professor, Dept. of Civil Engineering, Tomakomai National College of Technology, Hokkaido.

\*\*\*\* Professor, School of Technology, Dept. of Civil Engineering, Hokkaido University, Hokkaido.

FAILURE MECHANISM

Herein, the log-spihal failure mechanism as shown in Fig. 1 is taken as the local slope failure mode. The pseudo-static method is then applied to evaluate the seismic displacement and corresponding yield acceleration of a slope during an earthquake. In this method, the effect of an earthquake on a potential sliding mass is represented by an equivalent static horizontal force determined as the product of seismic coefficient factor  $K$ , and the weight of the potential sliding mass.

1. REVIEW OF THEORETICAL FORMULATION

In case of the previous theoretical analysis<sup>(1)</sup>, sliding surface occurs at the end side of surcharge load (Fig. 1), and then all surcharge load effect the slope collapse as we have supposed. But results of the experiments didn't always effect the our assumption, the slip line started at arbitrary point within the surcharge load or at the front side of surcharge load with like a parabolic curve shape face (Fig. 2) perpendicular to the slip line. So, on our assumption, we use stress distribution of Sadowsky (Fig. 3) between the load and the perfectly plastic semi-infinite body. Then, we have to analyze the

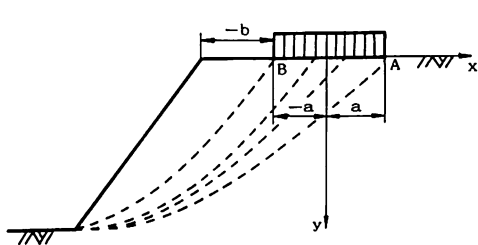


Fig. 1 Model of analysis

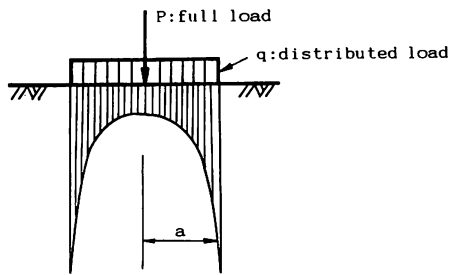


Fig. 3 Stress-Distribution by SADOWSKY

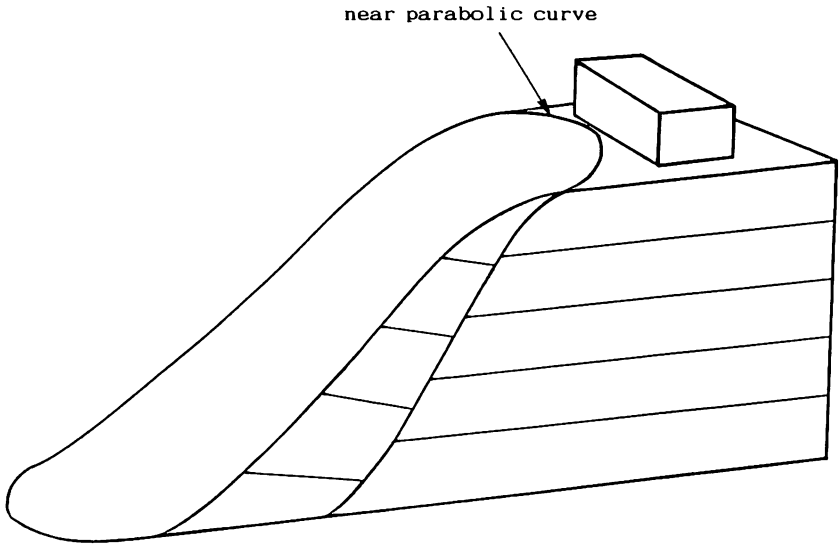


Fig. 2 Simplified Collapse of a Slope

two cases as follow :

- (1) Slip line occurs between the front of surcharge and center of surcharge (y-axis) ;  $-a < x < 0$
- (2) Slip line occurs between the y-axis and the end of sucharge ;  $0 < x < a$  (see Fig. 4, 5)

At a result, changing the terms of load as follow, we can analyze the same situation of the model tests (Fig. 5)

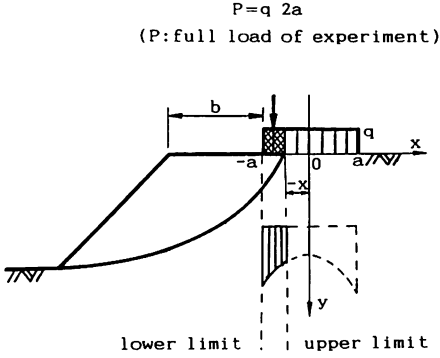


Fig. 4 Case of :  $-a < x < 0$

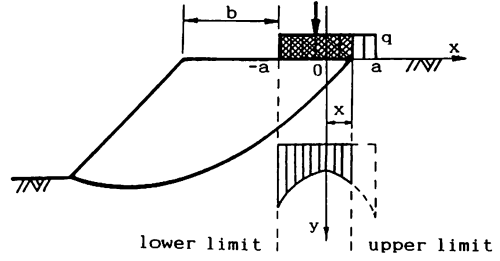


Fig. 5. Case of :  $0 < x < a$

case of  $-a < x < 0$

$$f_p = \frac{L}{\gamma_0} \left( \cos \theta_0 - \frac{L}{2\gamma_0} \right) \cdot \frac{1}{\pi} \left\{ \sin^{-1} \frac{-(a+x)}{a} + \frac{\pi}{2} \right\} \quad (1)$$

$$f_q = \frac{L}{\gamma_0} \sin \theta_0 \cdot \frac{1}{\pi} \left\{ \sin^{-1} \frac{-(a+x)}{a} + \frac{\pi}{2} \right\} \quad (2)$$

case of  $0 < x < a$

$$f_p = \frac{L}{\gamma_0} \left( \cos \theta_0 - \frac{L}{2\gamma_0} \right) \cdot \frac{1}{\pi} \left\{ \sin^{-1} \frac{x}{a} + \frac{\pi}{2} \right\} \quad (3)$$

$$f_q = \frac{L}{\gamma_0} \sin \theta_0 \cdot \frac{1}{\pi} \left\{ \sin^{-1} \frac{x}{a} + \frac{\pi}{2} \right\} \quad (4)$$

Newmark is the first to propose the important concept that the seismic stability of slopes should be evaluated from the viewpoint of displacements rather than the traditional minimum factor of safety<sup>(10)</sup>. To this end, Newmark demonstrated that a soil mass moving downward along a failure surface under an earthquake-induced inertia force is similar to that of a rigid block with weight and external force sliding along an inclined surface with friction.

Referring to Fig. 7 and Fig. 8, these show the case of  $K = K_c$  and case of  $K = K_i > K_c$ . We can obtain the angular acceleration ( $\ddot{\theta}$ ), the angular velocity ( $\dot{\theta}$ ) and the angular displacement ( $\theta$ ) as follow ;

$$\theta_{i+1} = \theta_i + \dot{\theta}_i(t_{i+1} - t_i) + \frac{(\ddot{\theta}_i + \ddot{\theta}_{i+1})(t_{i+1} - t_i)}{6} \quad (5)$$

$$\dot{\theta}_{i+1} = \dot{\theta}_i + \frac{(\ddot{\theta}_i + \ddot{\theta}_{i+1})(t_{i+1} - t_i)}{2} \quad (6)$$

$$\ddot{\theta} = \frac{(K_i - K_c)g[\gamma r_0^3(f_4 - f_5 - f_6) + Pr_0^2 f_q]}{W_3 \ell^2} \quad (7)$$

Also, can be calculated the arm ( $\ell$ ) which is the length from O to the center of gravity of the failure slope (Fig. 7 and 8) as ;

$$\ell = \frac{\sqrt{[\gamma r_0^3(f_1 - f_2 - f_3)]^2 + [\gamma r_0^3(f_4 - f_5 - f_6)]^2}}{W_3} \quad (8)$$

Herein,  $f_1 \sim f_6$  is presented in the previous papers<sup>(1,3)</sup>. Multiplying Eq.(6) by Eq.(8), These procedures will be performed to find the overall slope-slide displacement.

The flow chart of computer program is shown in Fig. 9.

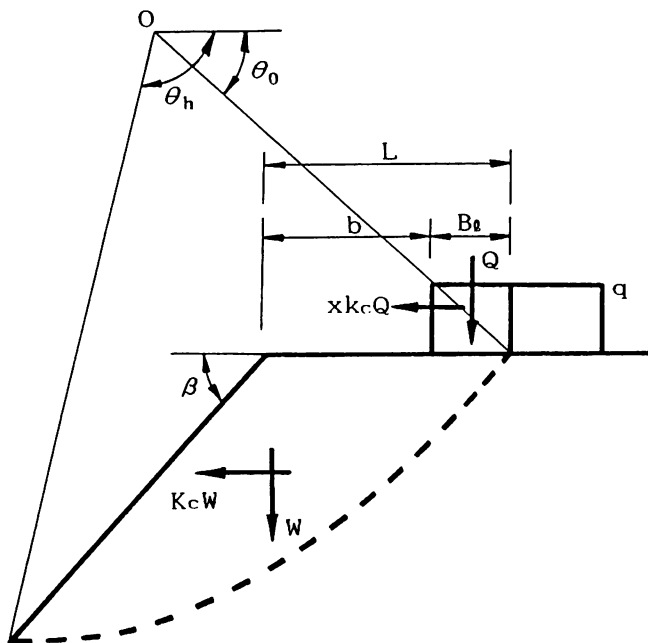


Fig. 6 Model of analysis

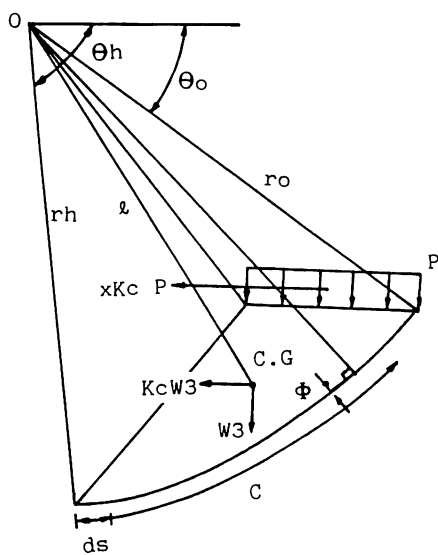


Fig. 7 Equilibrium of Force on Resting Block

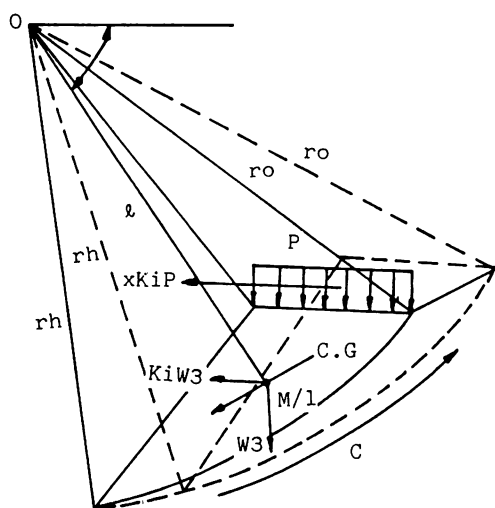


Fig. 8 Forces on Sliding Block

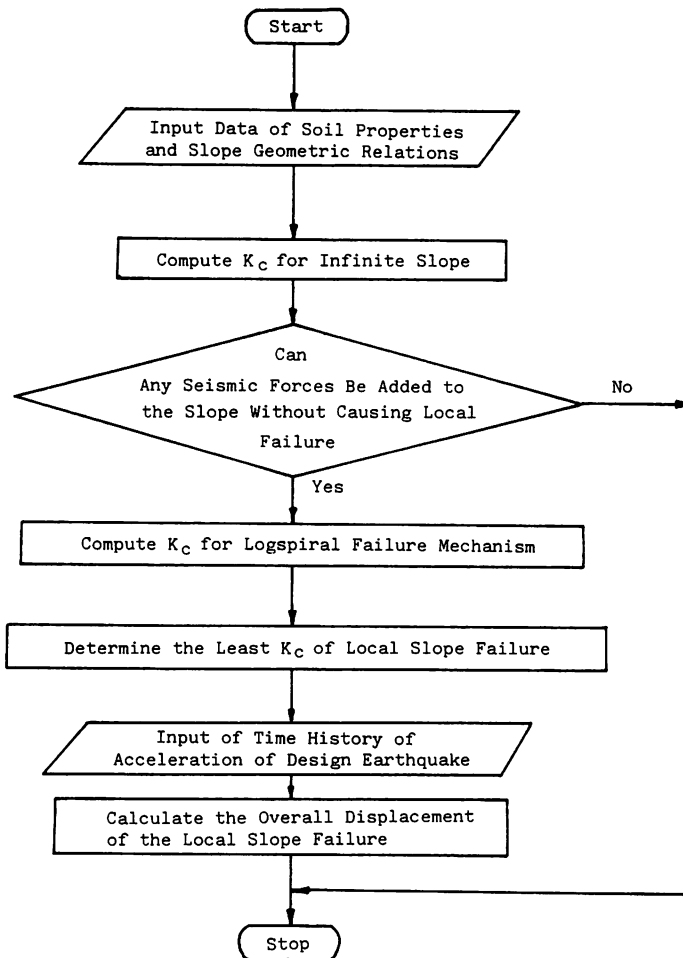


Fig. 9 Flow Chart of Computer Program

## 2. NUMERICAL RESULTS (Examples of Harmonic Earthquake Waves)

The following steps are used in the numerical studies.

1. Determine the critical failure mechanism and its corresponding yield acceleration at which slip just begins.
2. Based on the time-history of the acceleration of an actual or simulated earthquake, apply the pseudo-static forces to the slope.
3. When the induced acceleration exceeds the yield acceleration, rigid body type of slope movement will occur. The displacements are evaluated by intergrating all the positive velocities throughout the shaking of the earthquake.

A computer program was developed using the aforementioned analytical procedures.

The acceleration within a time interval is assumed to be linear but not necessarily constant. (Fig. 10 and 12) A harmonic earthquake program based on the aforementioned analytical procedue is developed. As an example, we determine the yield acceleration factor of the slope shown in Fig. 10 :

$K_c$  and its overall displacements under the harmonic earthquake shown in Fig. 10 and 11 where the angular acceleration, angular velocity and horizontal and vertical components of angular displacement  $\theta$  are given. Slip displacements occur when earthquakes exceed the yield acceleration of the slope: In these examples, cumulative displacement per unit-time vs. period is shown in Fig. 10~13 each of these is normalized by 0.204G respectively. In these figures, when the maximum earthquake acceleration getting larger, displacement per unit-time takes a large value. Various Periods also getting larger, displacements increase linearly with propotional to increment of period.

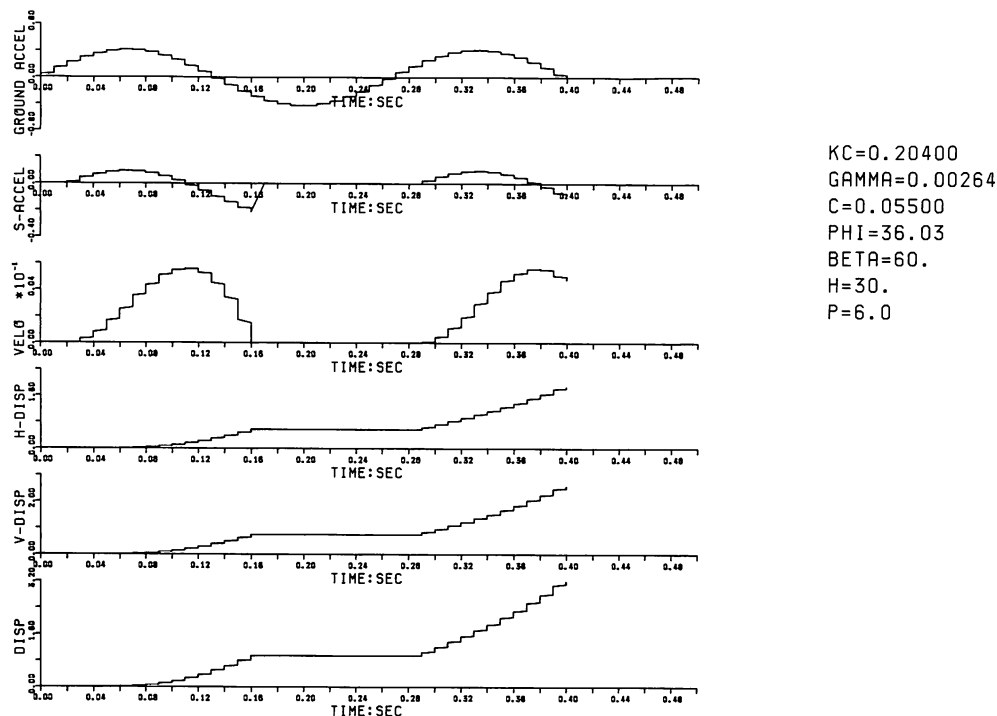


Fig. 10

### 3. EFFECTS OF MODEL TESTS

In this part, the model test of a slope collapse induced earthquake inertia force is described. This experimental investigation is conducted to study seismic sliding displacement and velocity of sliding mass in the laboratory. (Photo. 1)

In these tests, we equipped two sensors of acceleration. One of the sensors is buried in the model slope and other one is put the acrylic-test box as measuring acceleration of external horizontal inertia force (Photo. 1). As earthquake waves, we can put in nearly sine waves which have 2/3 Hz period 0.42G maximum acceleration. Thus, the signals are picked up by the sensors and they are measured through the dynamic strain meter, and we can find yield acceleration of slope with records of other data by a rapicorder. And the same time, we took the videotape of the seismic slope failure-experiments. So, we are able to understand slip displacement and slope-failure mechanism with the video tape of replaying. In this way, real displacement have to be calculated from posing replay pictures of video similar to exact model. Using Video-Replay-Machine, we can calculate the exact

displacements which similar to posing pictures in the video tape. And we can also find the interval times between the scene and the next scene by the machine. Then, we can measure sliding velocity with these two factors. Because of taking the photographs each scene, we can find failure mechanisms of the slope crealy (Photo. 2~7).

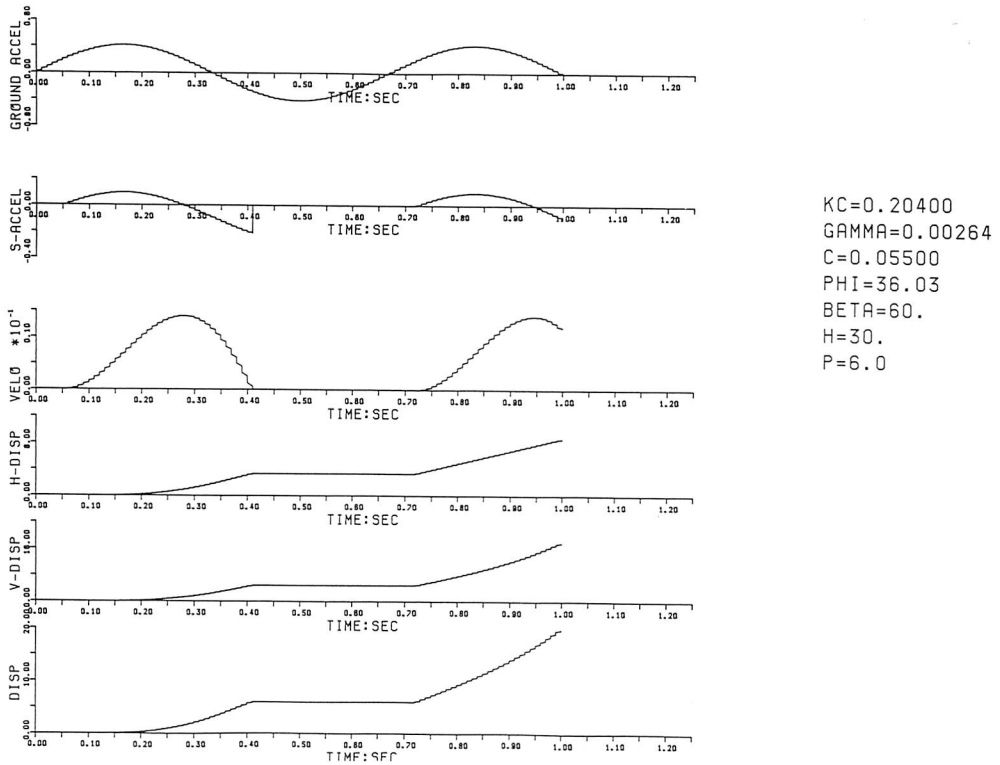


Fig. 11

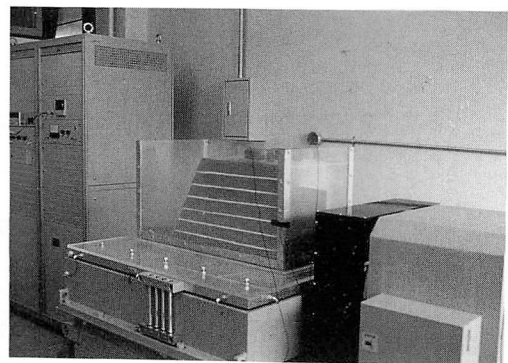
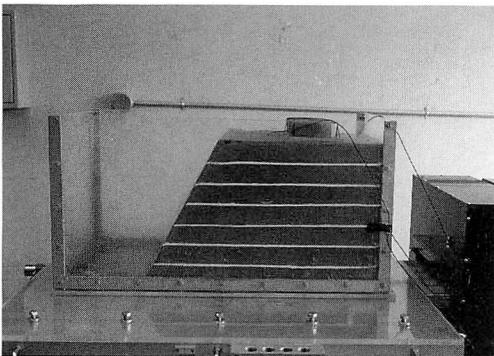


photo. 1 Model Test

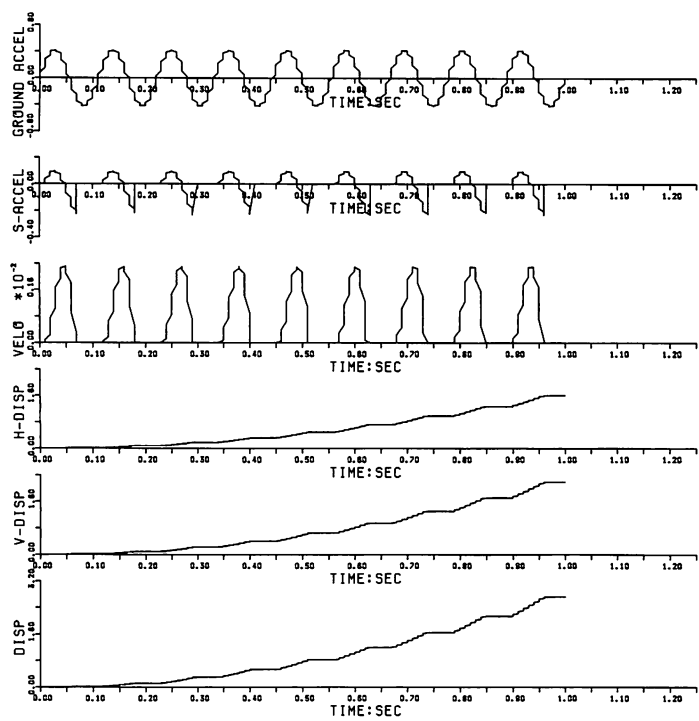
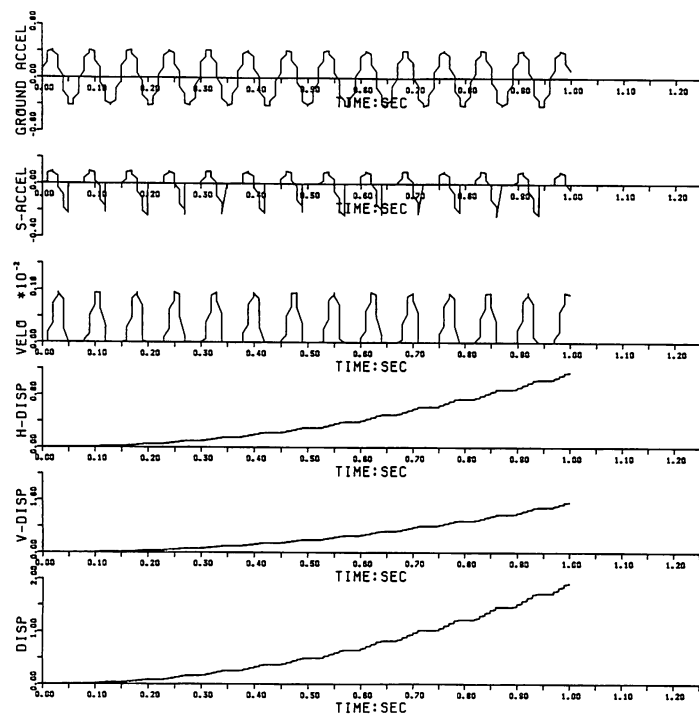


Fig. 12

KC=0.20400  
GAMMA=0.00264  
C=0.05500  
PHI=36.03  
BETA=60.  
H=30.  
P=6.0



KC=0.20400  
GAMMA=0.00264  
C=0.05500  
PHI=36.03  
BETA=60.  
H=30.  
P=6.0

Fig. 13



#### 4. COMPARISON EFFECTS OF THE TEST WITH NUMERICAL ANALYSIS

Between the effects of the tests (Table 1) and the effects of numerical analysis (Table 2 and Fig. 14), there is good agreement. So to speak, Table 1 shows that cumulative displacement is about 13.2 cm after 1.3 sec. of collapse starting in case of  $K_c = 0.204$ ,  $\beta = 60^\circ$ ,  $H = 35$  cm,  $P = 6$  kg and  $B = 10$  cm. In this Table 1,  $D_1 \sim D_4$  or  $V_1 \sim V_4$  means displacement and velocity of each observing point of the each line from the surcharge surface of the slope. Having almost same displacement at each point, the slope finish to collapse after 1.3 sec. from start to end. So, it seems to be similar to the assumption of the theoretical analysis which has behavior of a rigid body with a logarithmic spiral failure slide surface. (Photo 2~7) Similarly, the effect by numerical analysis added displacements of two waves exceeding  $K_c$  is also 13.54 cm. (Table 1) There is quite agreement among the former and latter. And then, numerical result of velocity have two peaks at the time of 0.24 sec. and 0.92 sec. after collapse

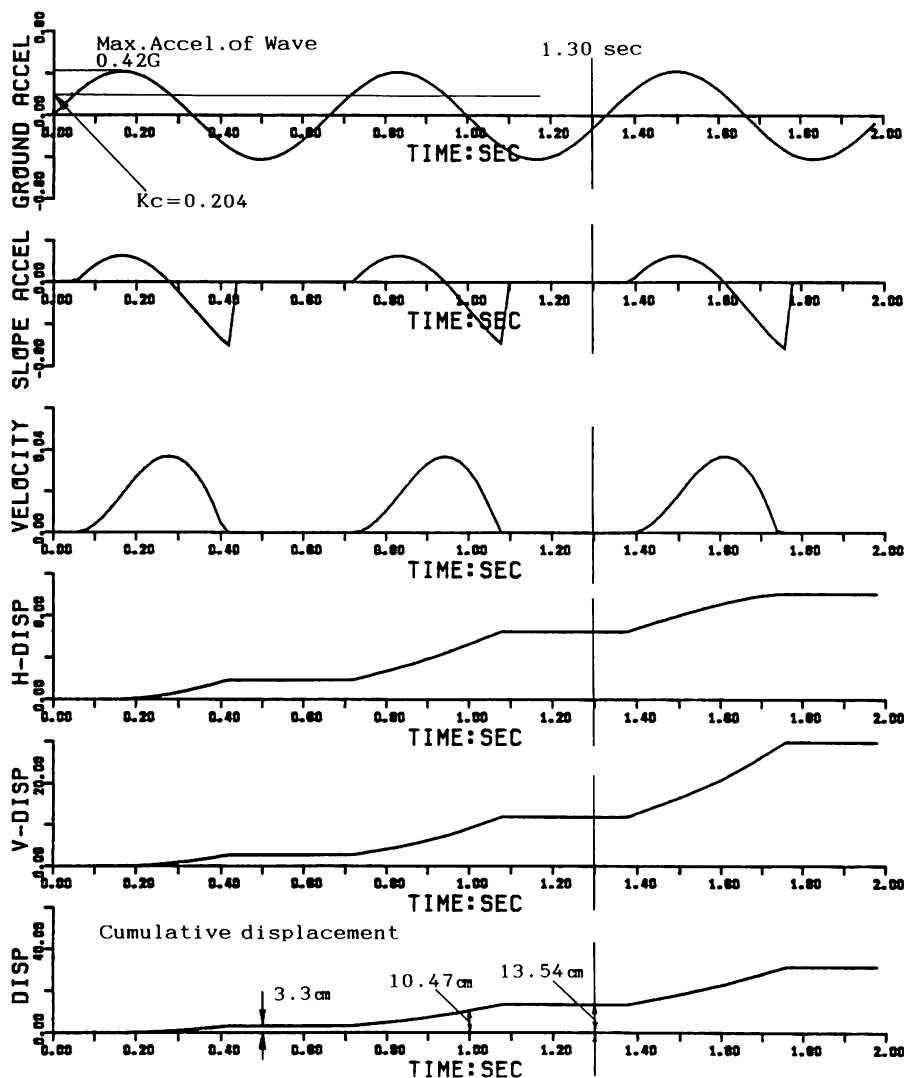


Fig. 14 Effect of numerical analysis

starting. (Fig. 14) On the other hand, the results of the test seems to have two peaks, too (Table 1). Generally speaking, the experiment and theoretical analysis is excellent agreement each other. We are able to investigate behavior of seismic slope-displacement crealy.

Table 1 Effects of Model Experiment

Time (sec)	Slide displacement Dl cm	Slide veiocity Vl cm/s	D2	V2	D3	V3	D4	V4
Callapase start right after	1.6	0.0	2.0	0.0	1.2	0.0	0.0	0.0
3/30	3.5	19.0	3.9	19.6	3.9	27.5	5.1	51.0
10/30	5.1	6.7	9.0	21.9	5.9	8.4	7.5	10.1
15/30	10.6	32.9	10.6	9.4	9.8	23.5	9.8	14.1
21/30	11.8	5.9	14.1	17.7	12.6	13.7	11.8	9.8
30/30	12.2	1.3	14.5	1.3	12.9	1.3	12.2	1.3
39/30	12.9	2.6	14.5	0.0	13.3	0.0	12.2	0.0

Table 2 Effects of calculation

Time (sec)	Accumulation slide displacement
0.10	0.004
0.50	3.305
1.00	10.468
1.30	13.541

SUMMARY AND CONCLUSIONS

The model developed in this study is based on a pseudo-static approach not a dynamic analysis, however, it can include the time history of the earthquake tremas.

In designing a slope, one may either adopt a procedure in which the static resistance of the slope is greater than the maximum earthquake acceleration likely to be encountered, or one can estimate the slope capacity in terms of accumulated displacements corresponding to those computed by the methods developed herein.

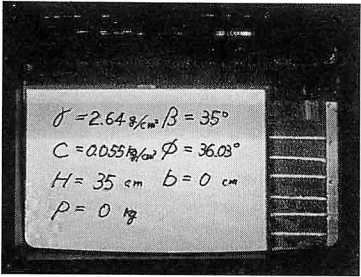
In some cases, it may be required to avoid permanent displacements altogether, that the value of yield acceleration be well in excess of the maximum earthquake acceleration. This appears to be too uneconomical a procedure for general use.

Comparison the effects of model tests with the effects of numerical analysis gives a quite good areement.

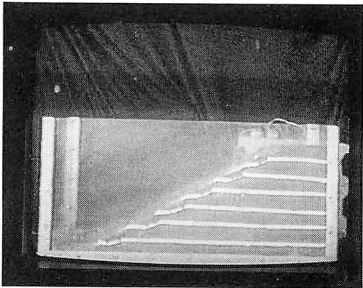
The shear strength of soils is known to be significantly influenced by the cyclic loading and the porewater pressure built-up is usually in an actual case. Taking this into account more studies.

The inclusion of these factors in a seismic analysis of slopes is necessary but complicated and should be considered in the further work.

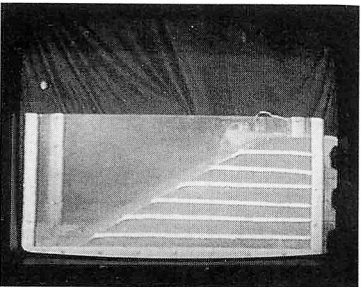
1. Express



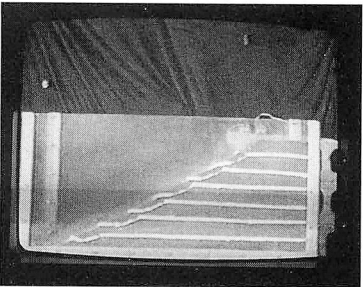
5. 51/30  
after  
minutes



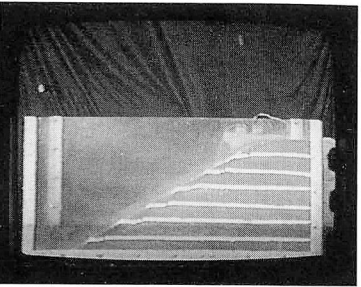
2. Collapse  
start just  
before



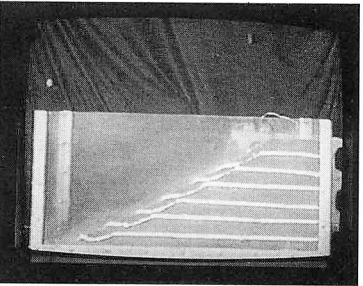
6. 118/30  
after  
minutes



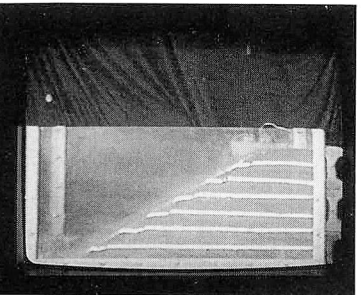
3. Collapse  
start right  
after



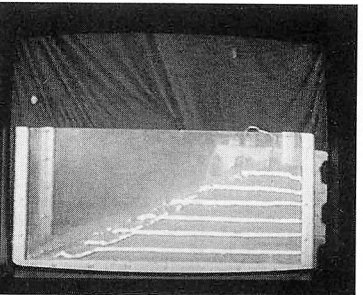
7. 173/30  
after  
minutes



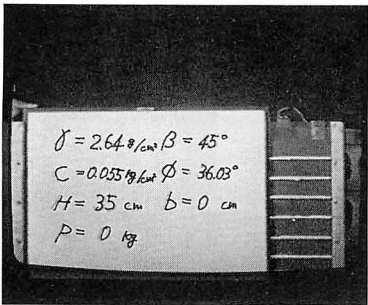
4. 9/30  
after  
minutes



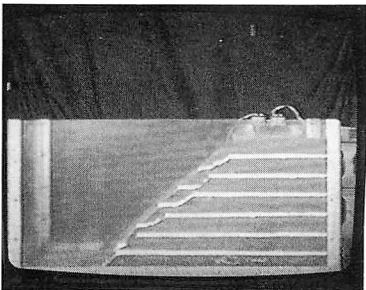
8. 24 after  
minutes  
collapse end



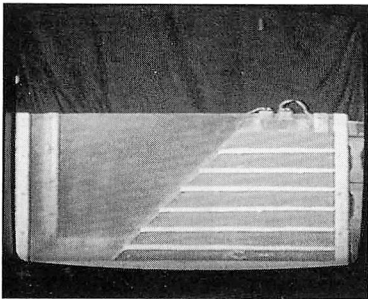
1. Express



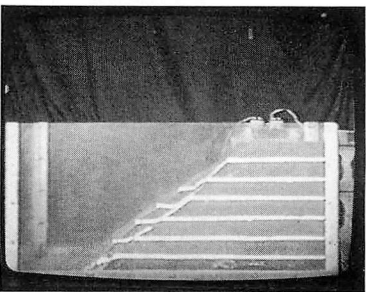
5. 14/30  
after  
minutes



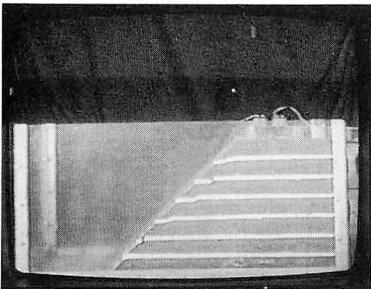
2. Collapse  
start just  
before



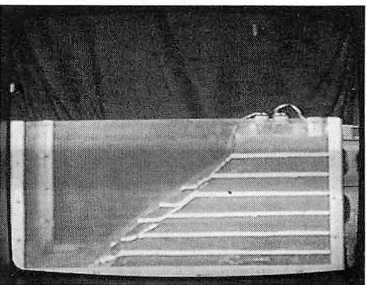
6. 28/30  
after  
minutes



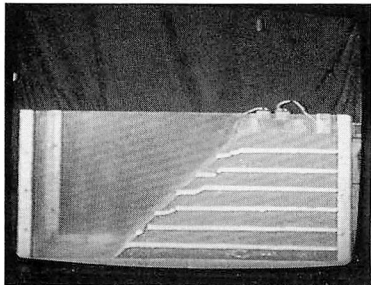
3. Collapse  
start right  
after



7. 47/30  
after  
minutes



4. 3/30  
after  
minutes



8. 99/30  
after  
minutes  
collapse end

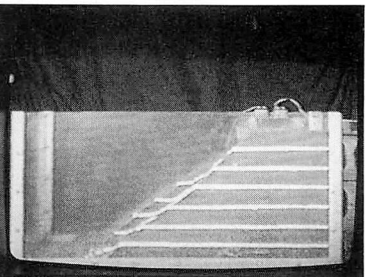
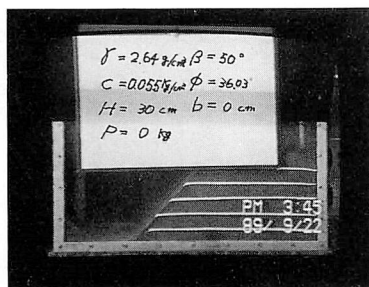
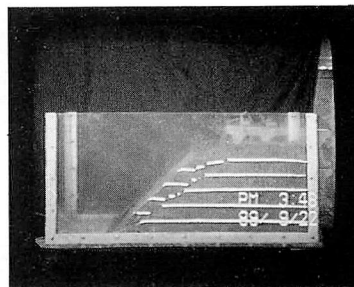


photo. 3

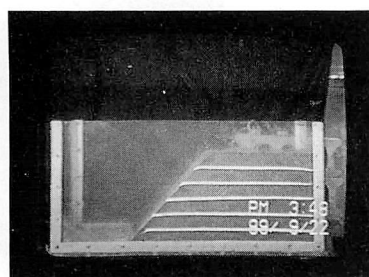
1. Express



5. 60/30  
after  
minutes



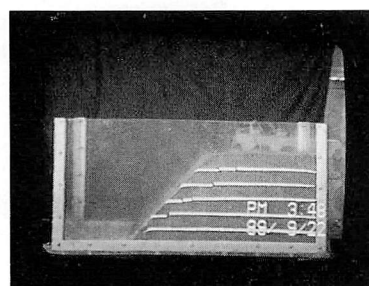
2. Collapse  
start just



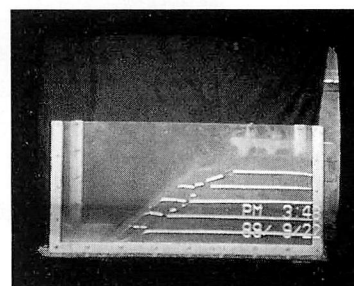
6. 90/30  
after  
minutes



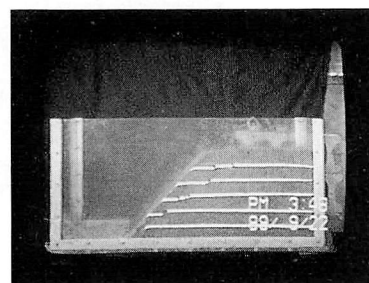
3. Collapse  
start right  
after



7. 195/30  
after  
minutes



4. 12/30  
after  
minutes



8. 215/30  
after  
minutes  
collapse end

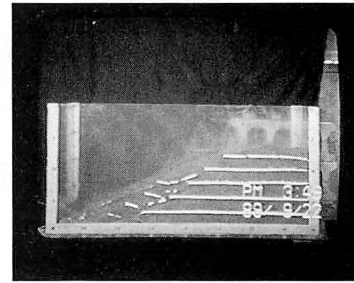
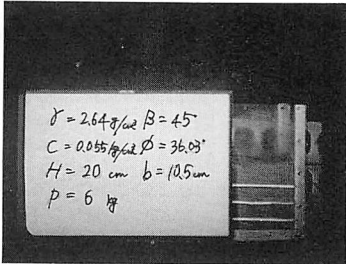
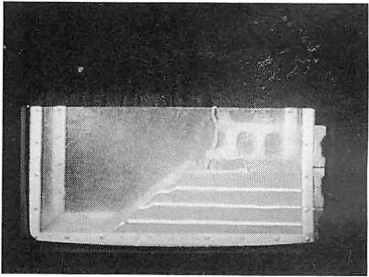


photo. 4

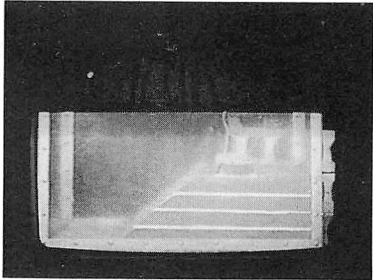
1. Express



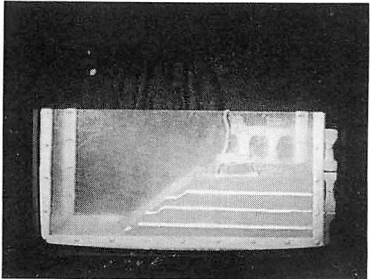
5. 10/30  
after  
minutes



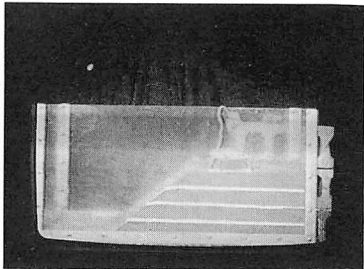
2. Collapse  
start just  
before



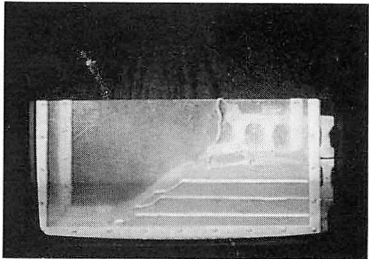
6. 24/30  
after  
minutes



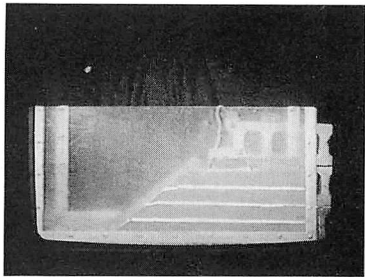
3. Collapse  
start right  
after



7. 66/30  
after  
minutes



4. 2/30  
after  
minutes



8. 105/30  
after  
minutes  
collapse end

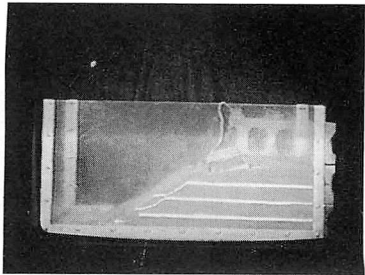
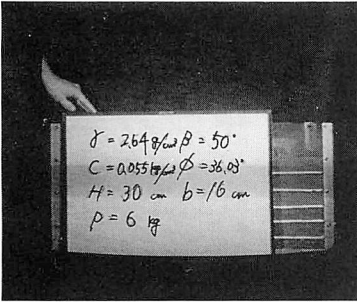
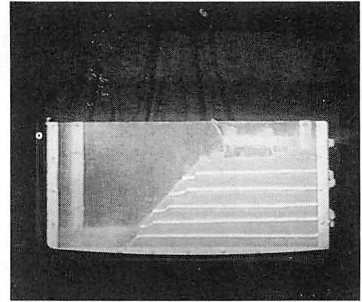


photo. 5

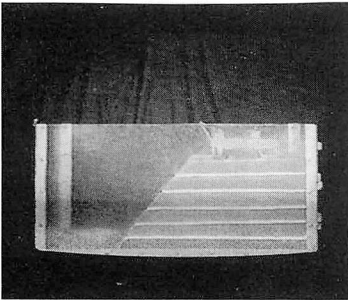
1. Express



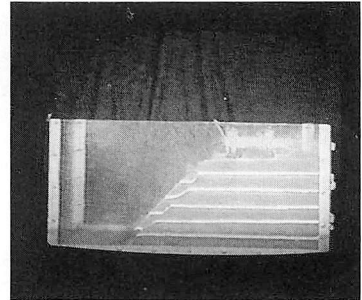
5. 19/30  
after  
minutes



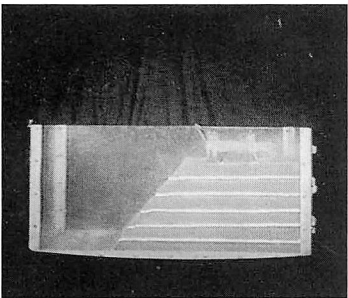
2. Collapse  
start just  
before



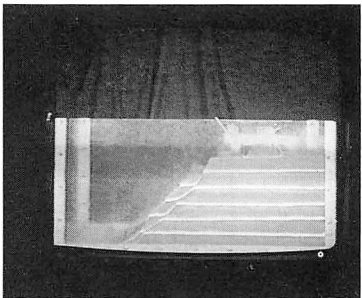
6. 22/30  
after  
minutes



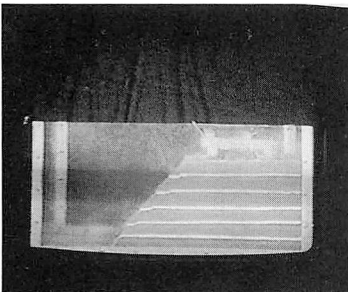
3. Collapse  
start right  
after



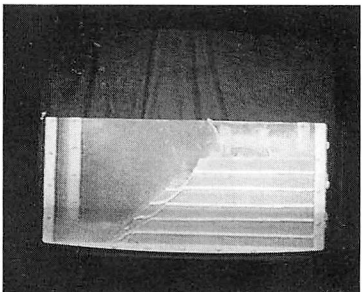
7. 32/30  
after  
minutes



4. 8/30  
after  
minutes

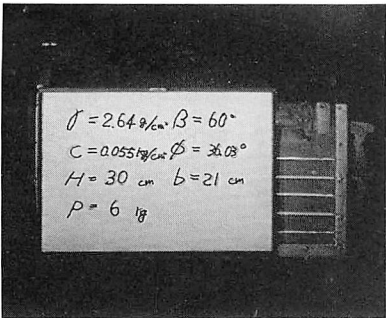


8. 167/30  
after  
minutes  
collapse end

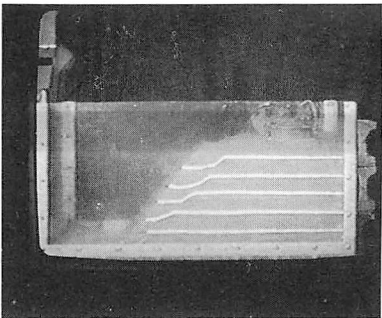




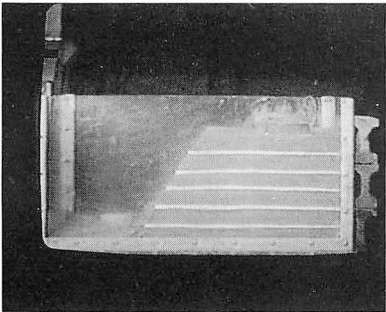
1. Express



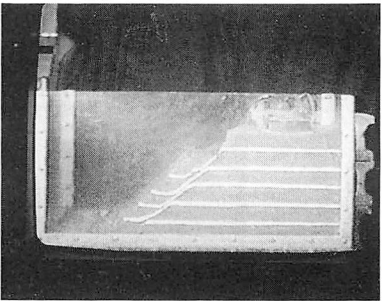
5. 8/30  
after  
minutes



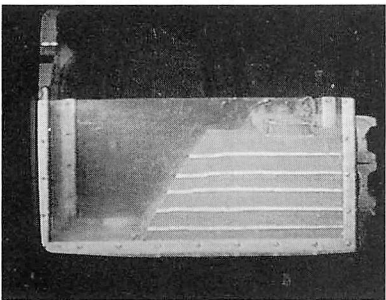
2. Collapse  
start just  
before



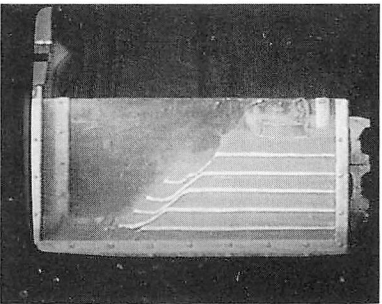
6. 18/30  
after  
minutes



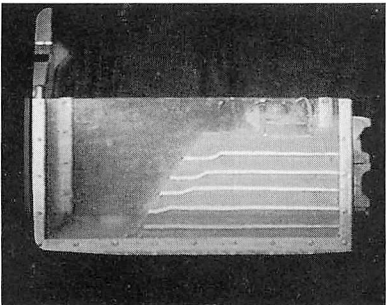
3. Collapse  
start right  
after



7. 48/30  
after  
minutes



4. 3/30  
after  
minutes



8. 108/30  
after  
minutes  
collapse end

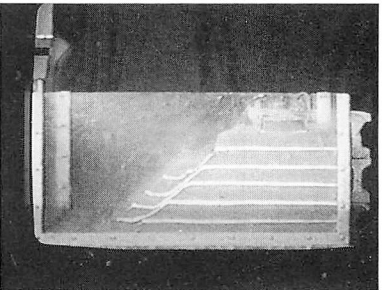


photo. 7



## ACKNOWLEDGMENTS

The authors deeply appreciate Kazutoshi SHIMODA and Jun FUJINUMA of the Tomakomai National College of Technology for the drawing Tables, Figures and the computational work.

## Appendix NOTATIONS

The following symbols are used in this paper ;

- $g$  : Acceleration of gravity.  
 $\gamma$  : Gravity of soil per unit volume.  
 $\gamma_0$  : Radius of rotational failure mechanism. (in Fig. 7)  
 $\phi$  : Internal friction angle.  
 $\theta_0$  : Angle of starting point of Log-spiral failure mechanism. (in Fig. 7)  
 $\theta_b$  : Angle of ending point of Log-spiral failure mechanism. (in Fig. 7)  
 $C$  : Cohesion strength.  
 $L$  : Length of failure mechanism.  
 $K_c$  : The yield (critical) acceleration factor.  
 $xK_c$  : The yield acceleration factor corresponding to the surcharge load  $P$  relating to the yield acceleration factor of the soil weight  $K_c$  multiplied by coefficient  $x$ , which can be greater or less than unity.  
 $\theta$  : Angle of slip failure mass of a slope.  
 $\dot{\theta}$  : Angular velocity of failure mass of a slope.  
 $\ddot{\theta}$  : Angular acceleration of failure mass of a slope.

## REFERENCES

1. Sawada, T., Nomachi, G. S., Ono, T. and Chen, W. F., "Model Test of Yield Acceleration Factor — $K_c$ — of a Foundation Near Down-Hill Slope Induced Dynamic Waves", MEMOIRS OF THE TOMAKOMAI NATIONAL COLLEGE OF TECHNOLOGY NO. 26, March 1991.
2. Chen, W. F. and Sawada, T., "Seismic Stability of Slopes in Nonhomogeneous, Anisotropic Soils, "Structural Engineering Report No. CE-STR-82-25, School Civil Engineering, Purdue University, West Lafayette, IN, June 1982, pp. 12~43.
3. Chen, W. F. and Sawada, T., "Earthquake-Induced Slope Failure in Nonhomogeneous, Anisotropic Soils," Soils and Foundation, Japanese Society of Soil Mechanics and Foundation Engineering, Vol. 23, No. 2, June, 1983, pp. 125—139.
4. Drucker, D. C. and Prager, W., "Soil Mechanics and Plastic Analysis or Limit Design," Quarterly of Applied Mathematics, Vol. 10, 1952, pp. 157—165.
5. Newmark, N. W., "Effects of Earthquakes on Dams and Embankments," The Fifth Rankine Lecture of The British Geotechnical Society, Geotechnique, England, Vol. XV, No. 2, 1965, pp. 137—160.
6. Sawada, T., Nomachi, S. G. and Chen, W. F., "Stability of Slope with Anisotropic Cohesion Strength against Earthquake," Theoretical and Applied Mechanics, Proceeding of the 33 rd Japan National Congress for Applied Mechanics, Vol. 33, 1983, pp. 417—432.
7. Sawada, T., Nomachi, S. G. and Chen, W. F., "Seismic Stability of Nonhomogeneous, Anisotropic Slope," Proceedings of the Fourth Engineering Mechanics Division Specialty Conference, ASCE, Vol. II. May 1983, pp. 1009—1012.

